NOTICE CONCERNING COPYRIGHT RESTRICTIONS

Calculation of Steam and Water Relative Permeabilities Using Field Production Data, With Laboratory Verification

Jericho L. P. Reyes, Chih-Ying Chen, Kewen Li and Roland N. Horne

Stanford Geothermal Program, Department of Petroleum Engineering
Stanford University, Stanford, CA, U.S.A.

Keywords

Steam-water relative permeability, production data, The Geysers, Salton Sea field, DOGGR database

ABSTRACT

The steam and water relative permeabilities at The Geysers and Salton Sea geothermal reservoirs were calculated from available production data. A method was used to estimate the relative permeability curves using Darcy's law from mass production rates of steam and water that are available from the DOGGR database. A verification was also conducted using data measured in laboratory steam-water flow experiments. The laboratory results show good agreement with the relative permeabilities calculated from a standard Darcy's Law approach. The water saturation estimated from the production data (i.e. the *flowing* water saturation) was found to be a significant underestimate compared to the in-place (*static*) saturation. From the laboratory experiments, the relationship between the flowing water saturation and the in-place water saturation was developed. The relative permeability curves inferred from field production data, corrected to static saturation, show a behavior that is very similar to that seen in laboratory experiments.

Introduction

There are two types of geothermal reservoirs: vapor-dominated reservoirs where steam is the principal recovery fluid and liquid-dominated reservoirs where liquid water is the principal recovery fluid. In both cases, the interaction between these two different phases has been the subject of numerous studies. Many measurements have encountered experimental difficulty due to phase changes during flow. An alternative way of determining how these two phases interact while in a state of flow would be very useful in the prediction of the ultimate recovery of the resource. Quantifying this interaction, by calculating the relative permeability of each of the phases, is of particular importance.

The objective of this study was to develop a method to calculate the relative permeabilities of steam and water by using production data from active geothermal fields, and to verify and calibrate this method using data from laboratory experiments. Knowledge of the relative permeabilities of steam and water will provide better understanding of the fluid flow interactions in the geothermal reservoir, and this is valuable in estimating the performance of a geothermal field and its capacity for further exploitation.

Background

There have been numerous attempts to characterize the steam and water relative permeability curves both experimentally and theoretically. The main difficulty of direct measurement has been the phase changes that occur during steam and water multiphase flow. A number of experiments have been made for nonboiling flow in fractured media, such as air-water (Diomampo, 2001) and water-oil. Current research on steam-water relative permeability in fractures (Chen *et al*. 2002, 2003) gives us a preliminary insight on the characteristics of the interaction of these two phases with one another.

The two most frequently used functions for relative permeability are the linear model (X-curve) and the Corey-model (Corey, 1954). These functions are dependent on phase saturation. The X-curve has a linear relationship with saturation:

$$k_{rl} = S_l \tag{1}$$

$$k_{rg} = S_g \tag{2}$$

where S_l and S_g are the liquid and gas saturation respectively. The Corey model is expressed as follows :

$$k_{rl} = S^{*4} \tag{3}$$

$$k_{rg} = (1 - S^*)^2 (1 - S^{*2}) \tag{4}$$

$$S^* = (S_l - S_{rl}) / (1 - S_{rl} - S_{rg}) \tag{5}$$

Chen et al. (2002) developed a method to compare steam- and air-water transport through fractured media. The main finding was that steam-water flow behavior in fractures is

different from that of nitrogen-water flow. Chen et al. (2003) found less phase interference in steam-water flow, and saw the behavior of the steam-water relative permeabilities behave closer to the X-curve.

The DOGGR Database has been made available publicly by the California Division of Oil, Gas and Geothermal Resources. The database contains production histories of, among others, the Geysers and Salton Sea geothermal wells. The data include temperature, pressure and steam and water production rates. These parameters were used in this study. The Geysers Geothermal Field, a vapor-dominated reservoir field, is located in Northern California about 130 km north of San Francisco. The Salton Sea Geothermal Field, a liquid-dominated reservoir field, is located in Imperial County in Southern California.

Method

Shinohara (1978) described a method to estimate the steam and water relative permeabilities in geothermal reservoirs, and applied this method to production data from the Wairakei geothermal field in New Zealand. This method is simple and useful, in that it only needs the production flow rate history and the temperature of the reservoir, as well as the ability to evaluate each well separately. Some of the assumptions of this method include:

(1) The pressure gradient is constant for a short time in each well.
(2) The product of permeability and flowing area is constant in each well.
(3) Fluid flow follows Darcy's Law.
(4) Flow to the well is predominantly horizontal.

Under these assumptions and from Darcy's law:

$$Q_w = \rho_w \frac{k}{\mu_w} k_{rw} A p' \tag{6}$$

$$Q_s = \rho_s \frac{k}{\mu_s} k_{rs} A p' \tag{7}$$

where Q is the mass flow rate, ρ is the density, μ is the dynamic viscosity, k_r is the relative permeability, k is the absolute permeability of the geothermal rock, A is the cross sectional area of flow, and p' is the pressure gradient. The subtitles w and s refer to water and steam respectively.

Dividing Equation 6 by Equation7 gives us:

$$\frac{Q_w}{Q_s} = \frac{\upsilon_s}{\upsilon_w} \frac{k_{rw}}{k_{rs}} \tag{8}$$

where υ is the kinematic viscosity.

Taking the sum of Equations 6 and 7 gives us:

$$Q = Q_w + Q_s = \left(\rho_w \frac{k_{rw}}{\mu_w} + \rho_s \frac{k_{rs}}{\mu_s} \right) kAp' : \left(\frac{k_{rs}}{\upsilon_s} \right) \left[1 + \left(\frac{Q_w}{Q_s} \right) \right] kAp' \tag{9}$$

where Q is the total of mass production rate of steam and water.

If we assume kAp' is constant in each well, then Equation 9 shows that a plot of Q vs Q_w/Q_s would be almost linear when Q_w/Q_s is small, and we can find the value of kAp' from either the intercept or the gradient of the line on the graph. This intercept, where $Q_w/Q_s = 0$, becomes Q^*, where:

$$Q^* = \frac{1}{\upsilon_s} kAp' \tag{10}$$

Because $k_{rs} = 1$ at $Q_w = 0$, then, substituting Equation 10 into Equation 6 and 7,

$$k_{rw} = \left(\frac{\upsilon_w}{\upsilon_s} \right) \left(\frac{Q_w}{Q^*} \right) \tag{11}$$

$$k_{rs} = \frac{Q_s}{Q^*} \tag{12}$$

Therefore knowing Q^*, we can calculate k_{rs} and k_{rw} by also knowing Q_w, Q_s, υ_s, and υ_w Unfortunately, the actual water saturation cannot be obtained in actual geothermal reservoirs. To estimate water saturation roughly using the production data only, the volumetric ratios can be used to infer the reservoir water saturation in the absence of residual saturation and for homogeneous flow of both phases. This estimated water saturation is called the *flowing* water saturation, and can be calculated from:

$$S_{w,f} = \frac{(1-x)\nu_w}{(1-x)\nu_w + x\nu_w} \tag{13}$$

where x is the mass fraction of steam and ν_w and ν_s is the specific volume of water and steam, respectively. This flowing saturation is often referred to as the *fractional flow*. It must be understood that the flowing saturation is different from the actual (in-place) saturation in a geothermal reservoir.

In the next section, we will describe the application of Shinohara's method to the production data from The Geysers and Salton Sea geothermal fields. After that, we will present a verification of Shinohara's method by applying it to laboratory data in which the steam-water relative permeabilities were already known. Comparison with the laboratory data also reveals the relationship between the flowing saturation and the actual (in-place) saturation.

Reservoir Applications

The production data in the Geysers and Salton Sea geothermal fields include temperature, pressure and steam and water production rates. In choosing the wells to be used in this study, a number of issues had to be addressed. First, for the vapor-dominated reservoir, we had to find data from wells that had both steam and water production. Of the 503 wells made available to us from The Geysers, only 25 produced water. Nine wells were ultimately used, as these wells had a sufficient number of readings for the calculation. Also, the first

assumption of Shinohara's method tells us that it is necessary to choose a short time period over which we can assume a constant pressure gradient. Since production data are usually intermittent in nature and often have periodic fluctuations, we had to find data sets that had significant stable periods. Of the 128 wells documented in the database that belong to the Salton Sea field operated by CalEnergy, we used six wells for our liquid-dominated case.

Figures 1 and 2 are examples of steam and water production histories from Coleman 4-5, a Geysers well, and IDD – 9, a well from the Salton Sea geothermal field. Well IDD-9 (Figure 2) from Salton Sea had zero production for much of its history. We chose an interval that we can assume to have a roughly constant pressure gradient. For this work we chose an interval from mid-1990 to late-1992. Choosing the time interval for the vapor-dominated well is much easier. We tried to omit extreme readings from our analysis, therefore the spike seen in 1986-1987 was not chosen as part of the range. For this work, we used a data interval from mid-1987 to 1989. Figures 3 and 4 show the Q vs Q_w/Q_s graphs for Coleman 5-5 and IDD – 9, respectively. The value of Q^* is inferred from the y-intercept value from the linear fit to the graph. Table 1 shows the Q^*

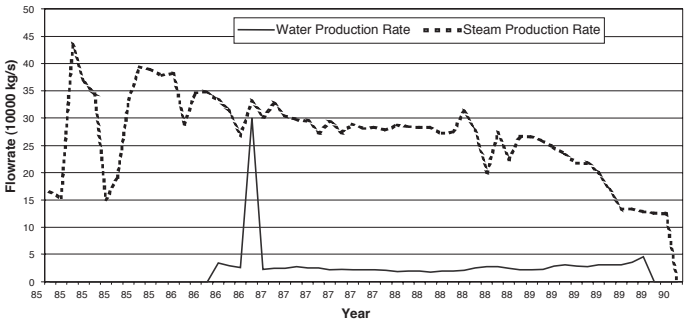

Figure 1. Steam and Water Production History of Coleman 4-5, The Geysers Geothermal Field.

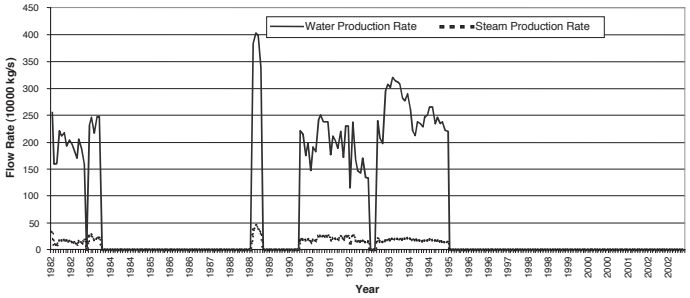

Figure 2. Steam and Water Production History of IID - 9, Salton Sea Geothermal Field.

inferred from all the wells used in the study.

If we compare the Q^* values between The Geysers wells and the Salton Sea wells, we can see that The Geysers' Q^* values are smaller than those from the Salton Sea. Also, The Geysers' Q^* values are close to each other. This is an extension of the second assumption made by Shinohara in developing his method. Not only is kAp' constant in a well, wells that are near each other or belong to the same geothermal field also have similar kAp' values. Since the wells in a certain geothermal field mainly have the same k values, and to a certain extent, A

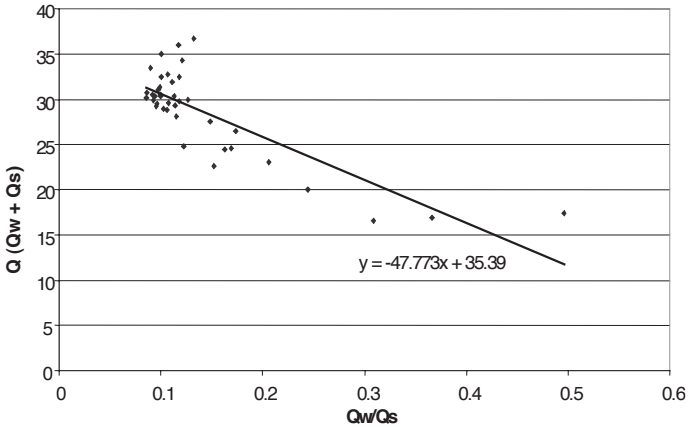

Figure 3. Q vs. Qw/Qs to infer Q* for Coleman 4-5, The Geysers Geothermal Field.

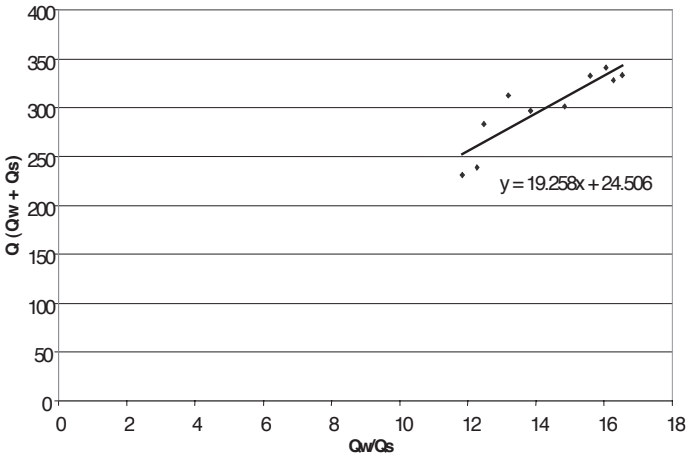

Figure 4. Q vs. Qw/Qs to infer Q* for IID - 9, Salton Sea Geothermal Field.

Table 1. Inferred Q* values for the Geysers and Salton Sea Geothermal Field Wells.

Geysers Wells	Q*	Salton Sea Wells	Q*
Coleman 4-5	35.39	IID – 9	100
Coleman 5-5	35.649	Sinclair 20	75
Coleman 3-5	24.186	Vonderahe 1	437.56
Francisco 2-5	24.182	Sinclair 10	298.62
Coleman 1A-5	24.09	Elmore 100	200
Thorne 6	33.59	Sinclair 11	256.5
Thorne 1	17.384		
Francisco 5-5	23.52		
CA-5636 6.8E-20	27.868		

and p', then our inferred values are consistent with each other. The Salton Sea wells have a wider range of values of Q*, but are generally of the same magnitude and larger than those in The Geysers. To evaluate the kinematic viscosities and mass production rates of the steam and water correctly, we must infer the bottomhole conditions, as these reflect the true flowing conditions of the well. We made temperature corrections based on the documented depths of the wells.

We can now use Equations 11 and 12 to calculate the relative permeabilities of steam and water. Figures 5 and 6 shows us a plot of relative permeability with water saturation for The Geysers and Salton Sea geothermal wells, respectively. Note that these graphs are plotted against the *flowing* saturation, $S_{w,f}$, as defined by Equation 13. The *flowing* saturation excludes the immobile water and steam fractions. The water saturation was estimated by using Equation 13 since the actual (in-place) water saturation was not available. Figure 5 shows The Geysers relative permeability plot. Because The Geysers is a vapor-dominated reservoir, we expected the low water saturation values. Figure 6, the Salton Sea examples, shows us a larger range for flowing water saturation, with a maximum at around 0.25. Even with a vapor-dominated reservoir, we see that, volumetrically, the steam saturation values still dominate, even if, by mass, water production is greater. We can see the general trend of the relative permeability curves by plotting both well samples into Figure 7. From Figure 7, we see that the relative permeability values for the vapor-dominated and liquid-dominated samples are only partially consistent with each other. For the relative permeability of steam, The Geysers calculation gives us a sharp drop in k_{rs} at small values of $S_{w,f}$. We then see a plateau of values approaching $S_{w,f} = 0.1$ from the Salton Sea values. For the relative permeability of water, we see a more constant and stable rise as the water saturation increases. The steepness of the rise for both sets of well samples is consistent. The water saturation in the figures seem to be much smaller than the traditional behavior of relative permeability curves, because of the use of flowing saturation based on Equation 13, rather than the true in-place saturation. A mapping between flowing and static water saturations based on laboratory experiment will be address in the next section.

To compare the estimated relative permeability values with the two most commonly assumed models of relative permeabilities, namely Corey and X curves, we plot the computed k_{rw} and k_{rs} values with these model curves in Figure 8. For The Geysers samples, we see that the relative permeability follows the Corey-model. On the other hand, the Salton Sea values lie more in the region between the X-curve and Corey-curve.

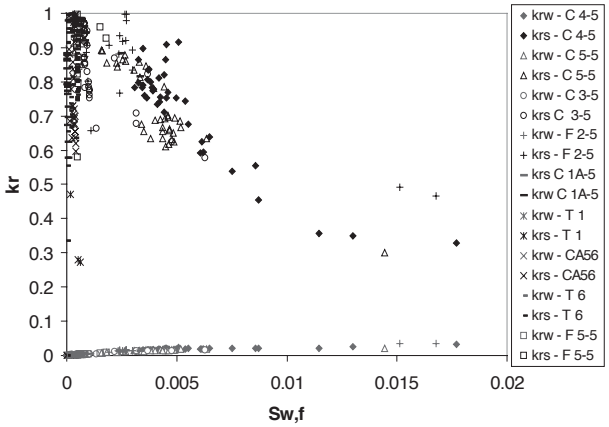

Figure 5. Plot of relative permeability curves against flowing water saturation for The Geysers Geothermal Field.

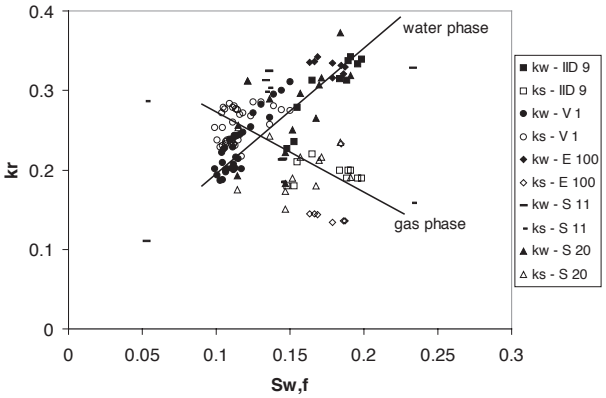

Figure 6. Plot of relative permeability curves against water saturation for the Salton Sea Geothermal Field.

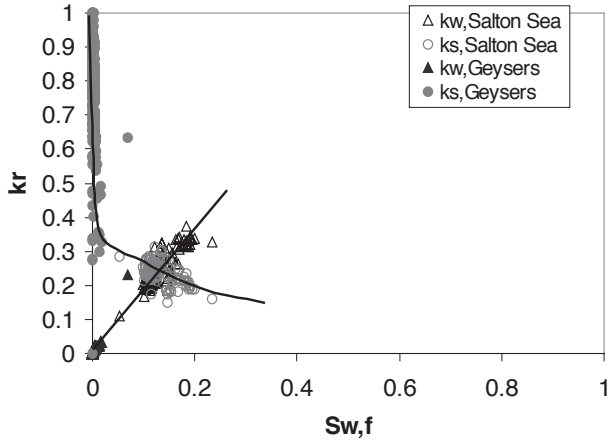

Figure 7. Plot of relative permeability curves against water saturation for The Geysers and Salton Sea Geothermal Reservoir Fields.

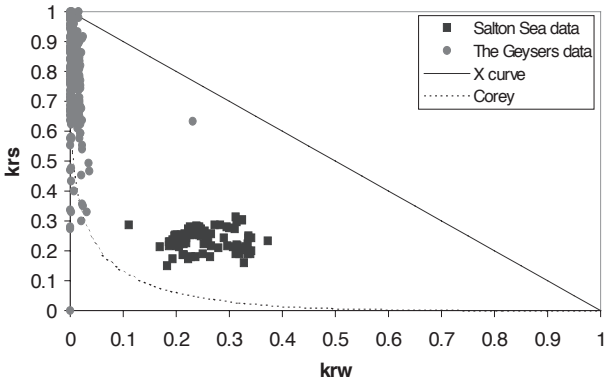

Figure 8. Plot of k_{rw} vs k_{rs} for The Geysers and Salton Sea Geothermal Field, with the Corey and X-curves.

We plot the data from Figure 8 again, this time with logarithmic axes, in Figure 9. We see from this graph that the calculated values lie between the X- and Corey-curves, for both The Geysers and Salton Sea wells.

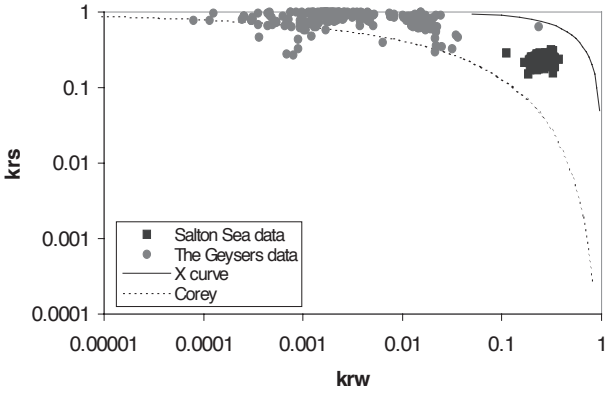

Figure 9. Logarithmic Plot of k_{rw} vs k_{rs} for The Geysers and Salton Sea Geothermal Field, with the Corey and X-curves.

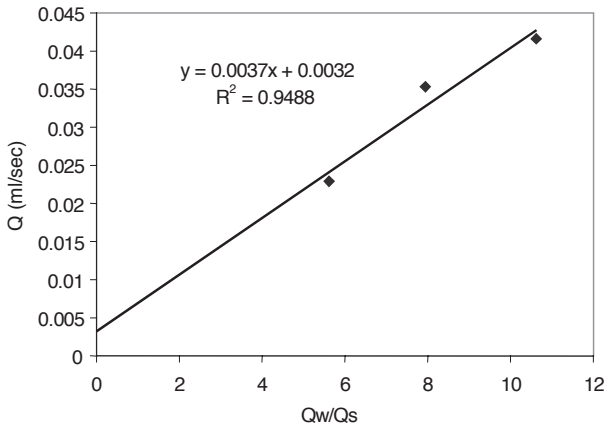

Figure 10. Q vs. Qw/Qs to infer Q* for the steam-water experiment of Chen et al. (2003).

Laboratory Verification

To confirm Shinohara's method and examine the relationship between the *flowing* saturation and the actual in-place (*static*) saturation, data from laboratory experiments were used. These data were obtained from steam-water flow experiments conducted by Chen *et al*. (2003). In these experiments, a FFRD (fractional flow ratio detector) device was used to sense both steam and water production rates. Flow visualization and image processing techniques were used to determine the water saturation (static), and differential pressure transducers were used to measure the pressure drop through the artificial reservoir (a single fracture). We used this "production data" from the laboratory to estimate relative permeabilities using Shinohara's method, and compared the results with those from the standard porous media approach provided by Chen *et al*. (2003).

Since the pressure gradient in the laboratory scale experiment was not constant, we scaled the data to a constant pressure gradient prior to the calculations. Figure 10 shows the Q vs. Q_w/Q_s plot in the experiment. The value of Q^* is 0.0032 ml/sec in this case. The steam-water relative permeabilities calculated from Shinohara's method (Equations 11 and 12) were compared with those from the porous media approach (Equation 6 and 7). A close agreement of relative permeability values from these two methods is shown in Figure 11. The steam-phase and water-phase values show less than 5% relative error between the two methods.

The relationship between flowing and static water saturations was examined by comparing the actual (static) water saturation measured in the experiment with the flowing water saturation calculated from Equation 13. From Figure 12, it is evident that the flowing water saturation is significantly less than the actual water saturation. The relationship between the two saturations can be expressed by a logarithmic trend as shown in Figure 13.

From Figures 11, 12 and 13 (12 and 13 overleaf), Shinohara's method can been seen to obtain accurate relative permeabilities if the reservoir pressure gradient is close to constant. However, the flowing saturation values inferred from Equation 13 are a significant underestimate of the static (in-place) saturation. The difference between the two saturations is due to the

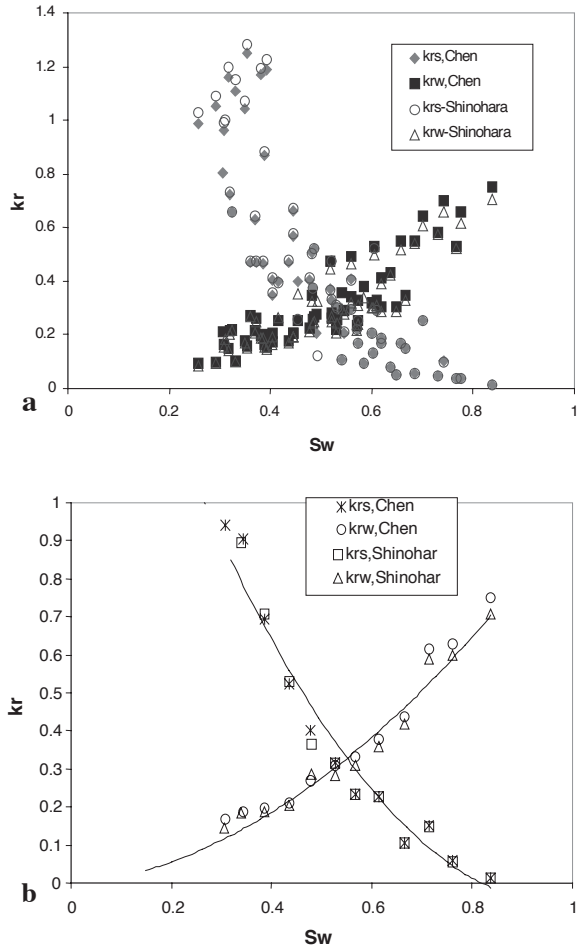

Figure 11. Comparison of steam-water relative permeabilities from porous media approach and Shinohara's method for the steam-water experiments: (a) generalized from five experimental runs; (b) averaged values.

velocity differences between steam and water phases, to the effects of immobile phases, and to the phase transformation effects. Therefore, we cannot simply use the flowing saturation to substitute for the real reservoir saturation. Figure 13b provides a mapping equation to relate the flowing and the actual

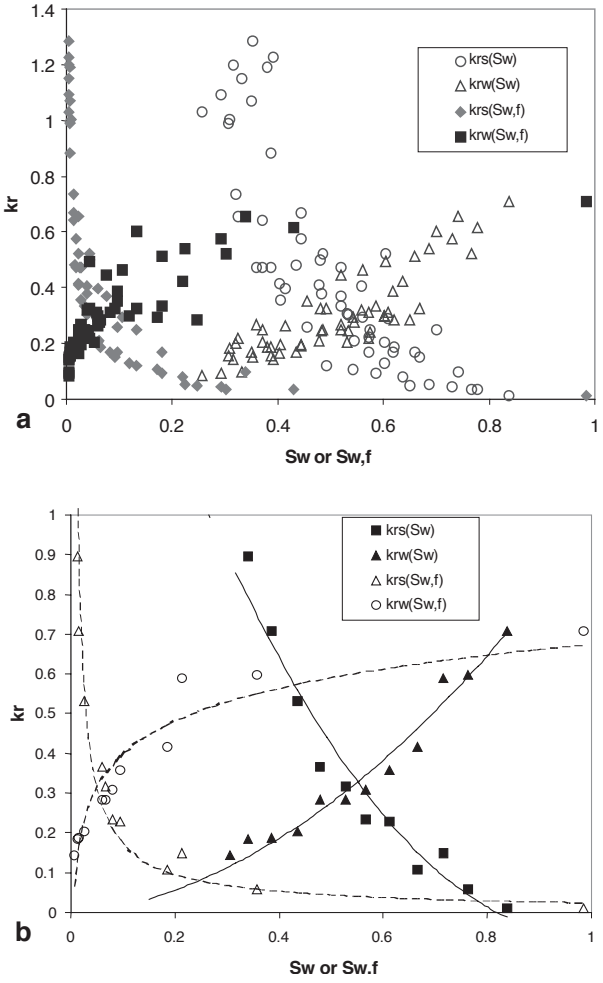

Figure 12. Comparison of kr vs. S_w and kr vs. $S_{w,f}$ from Shinohara's method for the steam-water experiments: (a) generalized from five experimental runs; (b) averaged values.

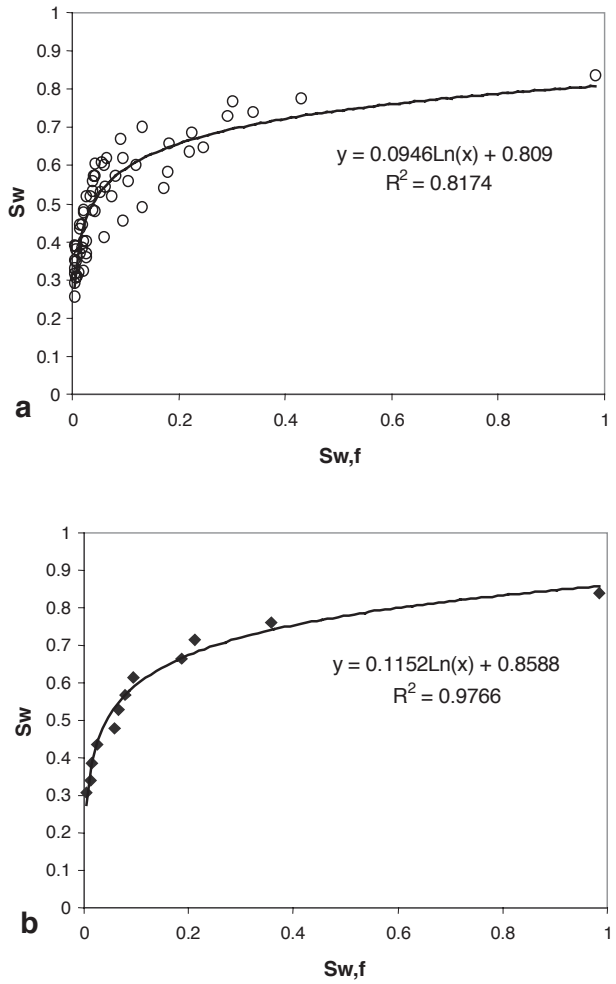

Figure 13. The flowing water saturation versus actual (static) water saturation: (a) generalized from five experimental runs; (b) averaged values.

water saturations for the laboratory scale measurements. The relationship between $S_{w,f}$ and S_w can be expressed as:

$$S_w = 0.1152 \ln(S_{w,f}) + 0.8588 \quad (14)$$

By applying Equation 14 to convert the (flowing) water saturation values estimated from both the Geysers and Salton Sea production data, Figure 7 can be replotted against the corrected (static) water saturation, as shown in Figure 14. Comparing Figure 14 with Figure 7, the underestimated water saturation has been improved, and Figure 14 shows more conventional relative permeability behavior. The relative permeabilities previously spanning from 0 to 0.23 (flowing) water saturation now range from 0 to 0.7 (static) water saturation after applying Equation 14. The solid curves in Figure 14 show the approximate trends of the relative permeability values for The Geysers and Salton Sea data, whereas the dashed lines are the trends for the experiments of Chen et al. (2003) shown earlier in Figure 13b. The estimates from the field production data still lie between the Corey and X-curves, and they are lower than the values measured by Chen et al. (2003). This observation

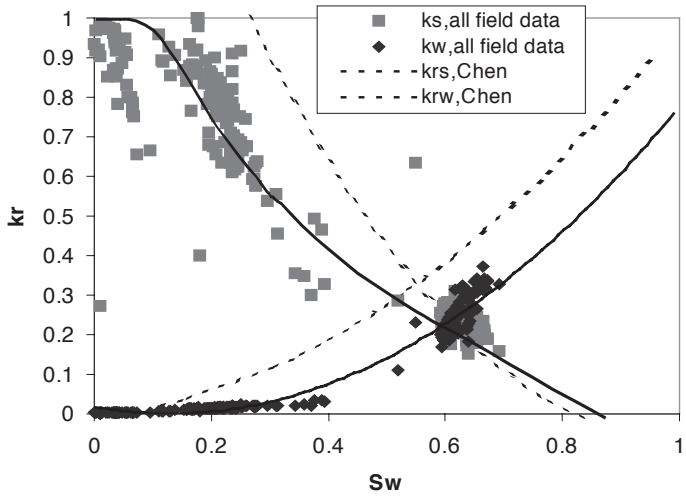

Figure 14. Relative permeability vs. mapped static water saturation from the field production data for The Geysers and Salton Sea Geothermal fields, compared to experimental results from Chen et al. (2003).

may imply more phase interference in the actual geothermal reservoirs, which is reasonable. Greater phase interference may be attributed to several issues. First of all, the fracture and matrix interaction was not included in Chen et al.'s single fracture apparatus. The surface morphology, the complexity of nature fracture network, and the wettability difference of the materials were not considered in the smooth-walled fracture model of Chen et al. (2003). Moreover, the scale difference may be important too. Nonetheless, the similarities between the two sets of curves are striking.

Conclusions

1) We can infer the steam and water relative permeabilities from field measurements of the production flow rate history and bottomhole temperature. Comparison with laboratory data demonstrated that this method can estimate the relative permeabilities accurately.
2) The estimated values of relative permeability in The Geysers and the Salton Sea geothermal fields lie between the X-curve and the Corey curve.
3) There is a sharp decline in the relative permeability of steam at small values of flowing water saturation, and this decline moderates as the saturation increases.
4) The relationship between the flowing water saturation and the actual (static) water saturation is close to logarithmic. After applying this correction, The k_r versus S_w curves from field data show a more conventional appearance.
5) In comparison to laboratory measurements from Chen et al. (2003), the estimated relative permeabilities from the field production data are lower, which implies that more phase interference occurs in the actual geothermal reservoirs.

References

Chen, C.-Y., Diomampo, G., Li, K. and Horne, R.N.: "Steam-Water Relative Permeability in Fractures," Geothermal Resources Council Transactions Vol.26, pp. 87-94, 2002.

Chen, C.-Y., Li, K. and Horne, R.N.: "Difference Between Steam-Water and Air-Water Relative Permeabilities in Fractures," Geothermal Resources Council Transactions Vol.27, pp. 793-800, Oct., 2003.

Corey, A.T., 1954. "The Interrelations Between Gas and Oil Relative Permeabilities," Producers Monthly, Vol. 19, p. 38-41.

Diomampo, G., "Relative Permeability through Fractures", MS report, Stanford University, Stanford, California (2001).

Shinohara, K., "Calculation and Use of Steam/Water Relative Permeabilities in Geothermal Reservoirs", MS report, Stanford University, Stanford, California (1978).